Extended Abstracts of the 1995 International Conference on Solid State Devices and Materials, Osaka, 1995, pp. 644-646

Modeling and Analysis of RF Plasma Using Electrical Equivalent Circuit

Kazuhide INO[1,2] and Tadahiro OHMI[1]

1) Department of Electronic Engineering, Faculty of Engineering, Tohoku University
Aza-Aoba, Aramaki, Aoba-ku, Sendai 980-77, Japan
2) Laboratory for Electronic Intelligent Systems, Research Institute of Electrical Communication, Tohoku University
2-1-1 Katahira, Aoba-ku, Sendai 980-77, Japan

The electrical equivalent circuits of RF plasmas have been obtained by use of the RF plasma direct-probing method and HSPICE simulation. Using the obtained equivalent circuits, the electrical characteristics of SF_6 and Ar plasmas have been compared. The SF_6 plasma displays sinusoidal waveform of the plasma potential for the capacitive sheath characteristics. On the other hand, in Ar plasma the displacement current through the grounded electrode sheath is comparable to the conduction (ion and electron) current. Then, the plasma potential in Ar plasma has significant higher harmonics for the non-linear characteristics of the grounded electrode sheath.

1. INTRODUCTION

RF plasma is of great importance and interest in a variety of applications, among which plasma processing is the best known and one of the most important technologies in the semiconductor manufacturing. In order to model the electrical characteristics of RF plasma using electrical equivalent circuits, quite a few approaches have been developed by many researchers[1-4]. Although the details of the various proposed circuits differ, the basic features are as shown in Fig. 1, that is described by resistors, diodes and capacitors. Unfortunately and mysteriously, no comparisons of the equivalent circuit shown in Fig. 1 with experimental data can be found in the literature. Then, the actual values of the circuit elements have not been experimentally clarified. Some measurements of various electrical parameters in RF discharges have been performed[3,4] in the past. To our knowledge, however, most experimental results are only compared with the simplified equivalent circuits such as the diode-omitted circuits. Therefore the purpose of this paper is to present the accurate electrical equivalent circuits by employing the RF plasma direct-probing method and the HSPICE simulation, and to analyze RF discharges by use of the obtained equivalent circuits.

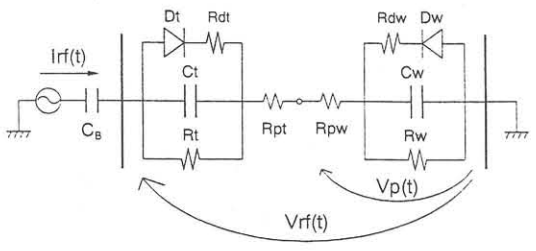

Fig. 1 Equivalent circuit model of RF discharges.

2. EXPERIMENTAL

The apparatus used in these experiments is illustrated in Fig. 2, that is a parallel-plate capacitively coupled RIE (Reactive Ion Etching) equipment with an excitation frequency of 13.56MHz. The diameter of electrodes is 20cm and the interelectrode distance is 4cm. RF power is supplied to the lower electrode through a parallel-plate line. The RF voltage waveforms appearing at the plasma excitation electrode were observed by an oscilloscope using a high voltage probe (Tektronix P6015). The probe was attached just below the electrode as shown in Fig. 2 to minimize stray impedance effects. The waveforms of RF current flowing through the plasma were also observed by an oscilloscope and a current probe. RF current can be obtained from the measurements of the uniform magnetic field between the parallel plates of the line by use of a coil. In addition, to precisely model the electrical characteristics of RF discharges, it is necessary to measure the waveforms of oscillating plasma potential. Then a plasma voltage probe was located centrally within the discharge, with their tips parallel to the electrode surfaces.

In general, it is possible to measure the time-averaged plasma potential by using a Langmuir probe, although it is required to avoid RF interferences in probe measurements[5]. The interferences are caused by the fluctuating voltage across the probe-plasma sheath. A general approach in making an undistorted probe measurements is to maximize the ratio of the probe-body impedance to the probe-sheath impedance. On the contrary, the measurements of the instantaneous plasma potential, that means the RF component of the plasma potential, is difficult. The instantaneous plasma potential has significant higher-order harmonics[6]. Then to achieve accurate measurements of the instantaneous plasma potential, it is required that the probe-body impedance is constant and much higher than the sheath impedance in both fundamental and higher-order harmonics. Godyak and Piejak has proposed[7] a capacitive probe to measure the instantaneous plasma potential. The probe makes it possible to measure the amplitude of the RF plasma potential with high accuracy, however, the direct-observation of the RF plasma potential is not possible due to low probe-body impedance compared to the sheath impedance.

In this study, we used a mesh probe[8,9] illustrated in Fig. 3 in order to observe the waveforms of oscillating plasma potential. The electrical equivalent circuit of the mesh probe is also described in Fig. 3. This probe has an aluminum mesh with a relatively large area (3cm × 3cm) in order to decrease the sheath impedance. Chip resistors (1kΩ × 5), which have

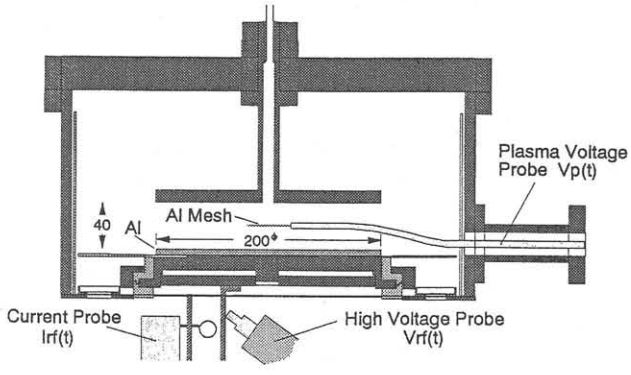

Fig. 2 Schematic diagram of experimental apparatus.

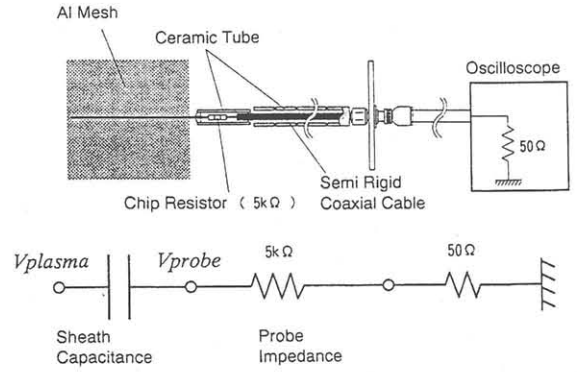

Fig. 3 Schematic diagram of a mesh probe for measurements of instantaneous plasma potential.

no dependence on frequency below 100MHz, are connected between the mesh and the probe body in order to increase the probe impedance. The series connection of 1kΩ chip resistors reduces the effect of parasitic capacitance of the resistors on the frequency characteristics of the probe impedance. The probe body is formed by a semi rigid coaxial cable with characteristic impedance of 50Ω. The cable is connected to an oscilloscope, whose input impedance is adjusted to 50Ω. Therefore the probe tip (i.e. the aluminum mesh) automatically follows the instantaneous plasma potential, and the waveform of the plasma potential can be observed on the oscilloscope. As a result, this probe acts as a passive voltage-probe with a signal attenuation of 101×.

By employing three types of probes shown in Fig. 2, the waveforms of RF voltage, RF current and the plasma potential were measured by an oscilloscope at the same time. The time-averaged plasma potential was also measured by an advanced Langmuir probe[8,9]. The measured waveforms were compared and fitted with those obtained by the HSPICE circuit simulation as described below.

3. RESULTS AND DISCUSSION

Figure 4 shows the measured waveforms of RF electrode voltage $V_{rf}(t)$, RF current $I_{rf}(t)$ and instantaneous plasma potential $V_p(t)$ of SF_6 discharge, where gas pressure and RF power were 150mTorr and 15W, respectively. These waveforms were compared with those obtained by the HSPICE circuit simulation using the equivalent circuit shown in Fig. 1. Figure 5 compares the measured and simulated waveforms in SF_6(a) and Ar(b) discharges, where gas pressure and RF power were 150mTorr and 15W, respectively. The equivalent circuits obtained by the simulation are also indicated. There are good agreements between the measured and simulated waveforms. Thus we can obtain the accurate

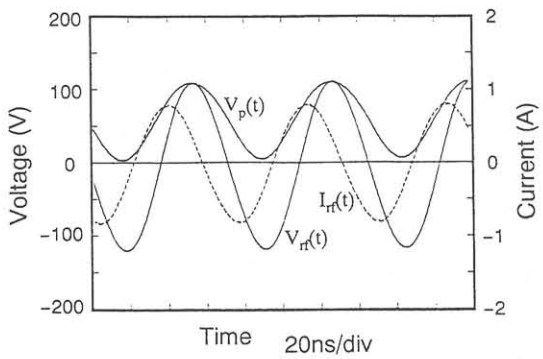

Fig. 4 Measured waveforms of RF electrode voltage $V_{rf}(t)$, RF current $I_{rf}(t)$ and instantaneous plasma potential $V_p(t)$ for SF_6 discharge.

electrical equivalent circuits of RF plasmas. The time-averaged plasma potential, which is one of the most important parameters in plasma processing, is lower in Ar discharge compared to SF_6 discharge. This is because the amplitude of $V_p(t)$ is lower in Ar discharge due to the lower sheath impedance adjacent to the grounded electrode than that of the RF electrode. In SF_6 discharge, the sheath impedances adjacent to each electrodes are comparable. Then the amplitude of $V_p(t)$ becomes about half of that of $V_{rf}(t)$. It is necessary to achieve lower time-averaged plasma potential in order to suppress the physical sputtering of chamber walls and resulting metal contamination. For this end, the sheath impedance adjacent to the grounded electrode should be lowered.

Figure 6 shows $V_{rf}(t)$ and $V_p(t)$ in the midplane and the sheath edges of each electrodes for an Ar discharge. The plasma excitation condition is identical with that of Fig. 5(b). These waveforms were obtained by the HSPICE simulation using the fitted equivalent circuit shown in Fig. 6. The amplitude and phase of the plasma potential are different at

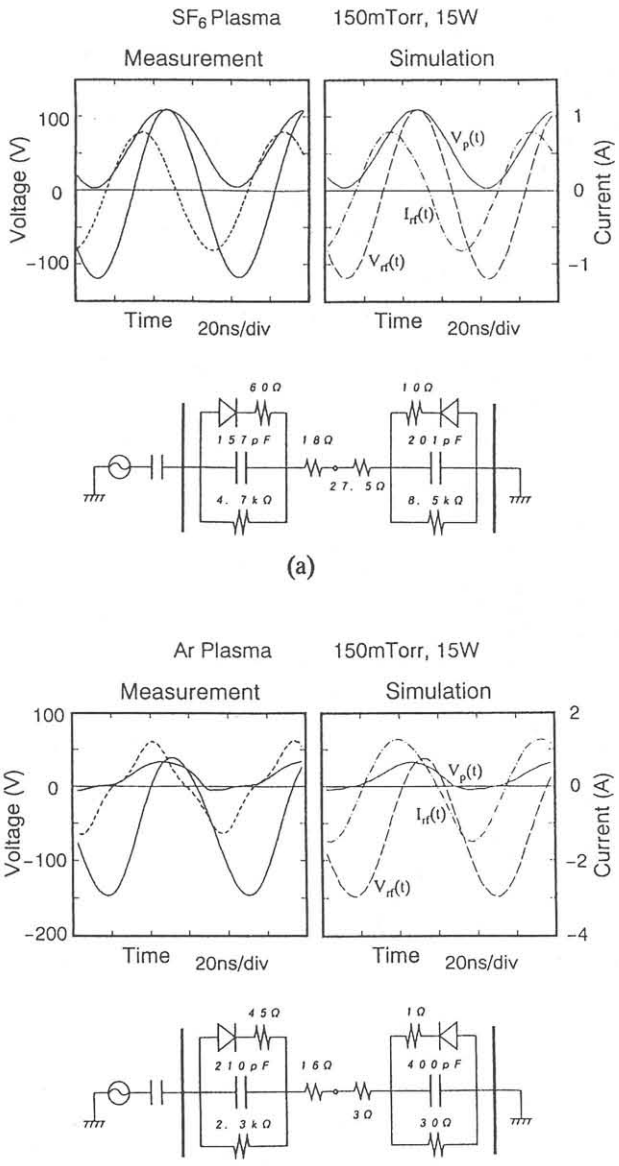

Fig. 5 Comparison of the measured and simulated waveforms of $V_{rf}(t)$, $I_{rf}(t)$ and $V_p(t)$ for (a)SF_6 and (b)Ar discharges. The equivalent circuits obtained by the simulation are also indicated.

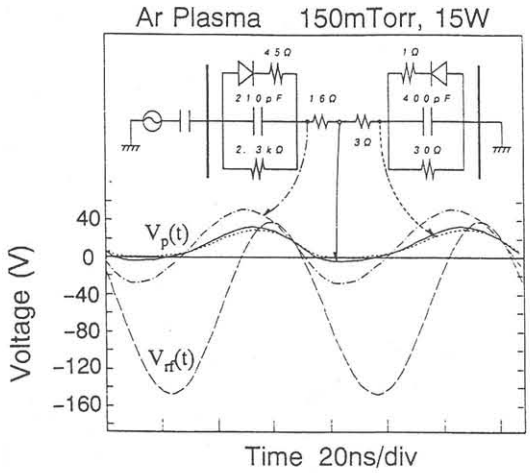

Fig. 6 $V_{rf}(t)$ and $V_p(t)$ in the midplane and the sheath edges of each electrodes for an Ar discharge.

each points due to the existence of the bulk plasma resistances R_{pt} and R_{pw}, that represent the electron heating in the plasma. By use of the equivalent circuit and the simulation, we can get the plasma potential everywhere in the plasma.

Figure 7(a) shows $V_{rf}(t)$, $I_{rf}(t)$ and $V_p(t)$ of SF_6 plasma, which are identical with those shown in Fig. 5(a). Figure 7(b)(c) show the current flowing through the sheaths adjacent to RF and grounded electrodes, respectively. I_d, I_i and I_e indicate the displacement current, ion current and electron current flowing through the sheaths, respectively. These waveforms were obtained by the HSPICE simulation using the equivalent circuit shown in Fig. 5(a). In SF_6 plasma, the displacement current through the RF and grounded electrode sheaths are much larger than the conduction (ion and electron) current. The SF_6 plasma displays sinusoidal waveform of the plasma potential shown in Fig. 5(a) for the capacitive sheath characteristics.

Figure 8(a) shows $V_{rf}(t)$, $I_{rf}(t)$ and $V_p(t)$ of Ar plasma, which are identical with those shown in Fig. 5(b). Figure 8(b)(c) show the currents I_d, I_i and I_e flowing through the sheaths adjacent to RF and grounded electrodes, respectively. These waveforms were obtained by the HSPICE

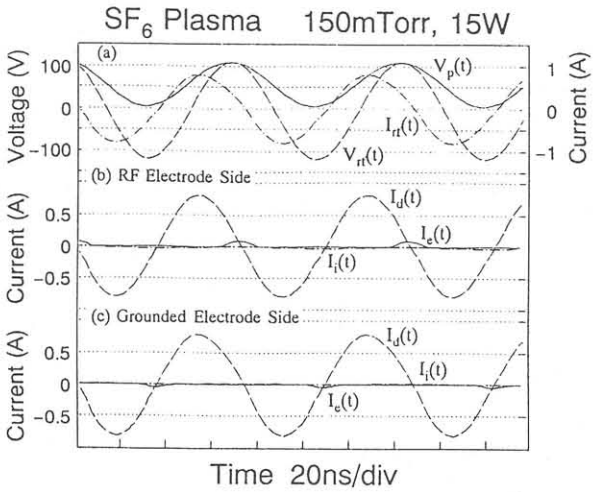

Fig. 7 (a) $V_{rf}(t)$, $I_{rf}(t)$ and $V_p(t)$ of SF_6 plasma, which are identical with those shown in Fig. 5(a). (b),(c) Current flowing through the sheaths adjacent to RF and grounded electrodes, respectively. I_d, I_i and I_e show the displacement current, ion current and electron current flowing through the sheaths, respectively.

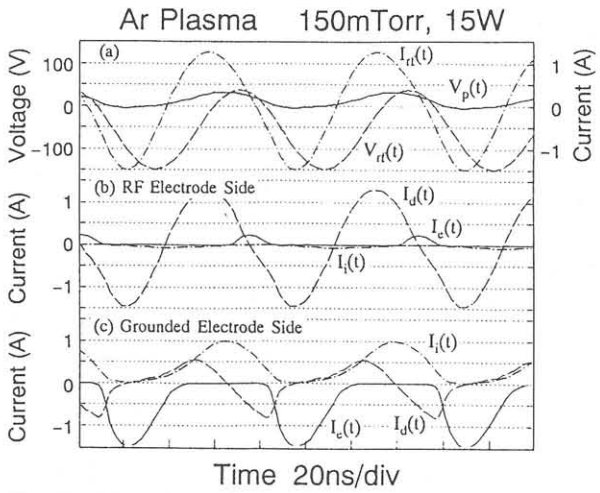

Fig. 8 (a) $V_{rf}(t)$, $I_{rf}(t)$ and $V_p(t)$ of Ar plasma, which are identical with those shown in Fig. 5(b). (b),(c) Current flowing through the sheaths adjacent to RF and grounded electrodes, respectively.

simulation using the equivalent circuit shown in Fig. 5(b). It can be clearly seen from this graph that the sheath current components are quite different between both sheaths in Ar plasma. In the case of RF electrode sheath, the main current flowing through the sheath is the displacement current due to the higher sheath resistance R_t. In the case of grounded electrode sheath, the ion and electron currents are comparable to the displacement current due to the lower sheath resistance R_w. The increased conduction current induces the distortion of the waveform of $V_p(t)$ as shown in Fig. 5(b) due to the non-linear characteristics of the grounded electrode sheath. The distortion also has an effect of lowering the time-averaged plasma potential.

4. CONCLUSION

The electrical equivalent circuits of RF plasmas have been obtained by use of the accurate probe measurements and HSPICE simulation. Using the obtained equivalent circuits, the electrical characteristics of SF_6 and Ar plasmas have been compared. The SF_6 plasma displays sinusoidal waveform of the plasma potential for the capacitive sheath characteristics. On the other hand, in Ar plasma the displacement current through the grounded electrode sheath is comparable to the conduction current. Then, the plasma potential in Ar plasma has significant higher harmonics for the non-linear characteristics of the grounded electrode sheath.

This analysis method will serve as an essential tool for modeling RF plasma.

References

1) H. R. Koenig and L. I. Maissel, IBM J. Res. Develop. **14** (1970) 168.
2) B. Chapman, *Glow Discharge Processes*, Wiley-Interscience, New York (1980) 169.
3) V. A. Godyak, R. B. Piejak, and B. M. Alexandrovich, IEEE Trans. Plasma Science **19** (1991) 660.
4) C. Beneking, J. Appl. Phys. **68** (1990) 4461.
5) A. P. Paranjpe, J. P. McVittie and S. A. Self, J. Appl. Phys. **67** (1990) 6718.
6) R. R. J. Gagne and A. Cantin, J. Appl. Phys. **43** (1972) 2639.
7) V. A. Godyak and R. B. Piejak, J. Appl. Phys. **68** (1990) 3157.
8) M. Hirayama and T. Ohmi, *Ext. Abst. SSDM*, Yokohama (1994) 697.
9) K. Ino, I. Natori, A. Ichikawa, and T. Ohmi, Jpn. J. Appl. Phys. **33** (1994) 505.